



Band gaps in bubble phononic crystals

Vincent Leroy, A Bretagne, M Lanoy, A Tourin

► To cite this version:

Vincent Leroy, A Bretagne, M Lanoy, A Tourin. Band gaps in bubble phononic crystals. AIP Advances, 2016, 6 (12), pp.121604. 10.1063/1.4968616 . hal-01470456

HAL Id: hal-01470456

<https://hal.sorbonne-universite.fr/hal-01470456>

Submitted on 17 Feb 2017

HAL is a multi-disciplinary open access archive for the deposit and dissemination of scientific research documents, whether they are published or not. The documents may come from teaching and research institutions in France or abroad, or from public or private research centers.

L'archive ouverte pluridisciplinaire **HAL**, est destinée au dépôt et à la diffusion de documents scientifiques de niveau recherche, publiés ou non, émanant des établissements d'enseignement et de recherche français ou étrangers, des laboratoires publics ou privés.



Distributed under a Creative Commons Attribution 4.0 International License

Band gaps in bubble phononic crystals

V. Leroy, A. Bretagne, M. Lanoy, and A. Tourin

Citation: *AIP Advances* **6**, 121604 (2016); doi: 10.1063/1.4968616

View online: <http://dx.doi.org/10.1063/1.4968616>

View Table of Contents: <http://aip.scitation.org/toc/adv/6/12>

Published by the *American Institute of Physics*

Articles you may be interested in

[Asymmetric propagation using enhanced self-demodulation in a chirped phononic crystal](#)

AIP Advances **6**, 121601 (2016); 10.1063/1.4968612

[Integrated phononic crystal resonators based on adiabatically-terminated phononic crystal waveguides](#)

AIP Advances **6**, 121603 (2016); 10.1063/1.4968614

[Multimodal and omnidirectional beam splitters for Lamb modes in elastic plates](#)

AIP Advances **6**, 121602 (2016); 10.1063/1.4971213

[Dynamic homogenization of viscoelastic phononic metasolids](#)

AIP Advances **6**, 121705 (2016); 10.1063/1.4968618

HAVE YOU HEARD?

Employers hiring scientists and
engineers trust

PHYSICS TODAY | JOBS

www.physicstoday.org/jobs



Band gaps in bubble phononic crystals

V. Leroy,¹ A. Bretagne,² M. Lanoy,² and A. Tourin^{2,a}

¹CNRS, Laboratoire Matière et Systèmes Complexes, University Paris Diderot, Sorbonne Paris Cité, F-75013 Paris, France

²CNRS, ESPCI Paris, PSL Research University, Institut Langevin, F-75005 Paris, France

(Received 30 August 2016; accepted 5 November 2016; published online 5 December 2016)

We investigate the interaction between Bragg and hybridization effects on the band gap properties of bubble phononic crystals. These latter consist of air cavities periodically arranged in an elastomer matrix and are fabricated using soft-lithography techniques. Their transmission properties are affected by Bragg effects due to the periodicity of the structure as well as hybridization between the propagating mode of the embedding medium and bubble resonance. The hybridization gap survives disorder while the Bragg gap requires a periodic distribution of bubbles. The distance between two bubble layers can be tuned to make the two gaps overlap or to create a transmission peak in the hybridization gap. © 2016 Author(s). All article content, except where otherwise noted, is licensed under a Creative Commons Attribution (CC BY) license (<http://creativecommons.org/licenses/by/4.0/>). [<http://dx.doi.org/10.1063/1.4968616>]

I. INTRODUCTION

A gas bubble in a liquid is an oscillator, much like a bob on a spring, that resonates at a natural frequency referred to as the Minnaert frequency: $\omega_0 = 1/R_0 \sqrt{3B_g/\rho_w}$ where B_g is the longitudinal modulus of the gas, ρ_w the mass density of the liquid, and R_0 the bubble radius.¹ This formula tells us that the restoring force is the elasticity of the gas while the inertia is that of the moving liquid. From here comes the particular status of the Minnaert resonance in acoustics: it is associated to a wavelength in water 500 times larger than the bubble radius. When a planar acoustic wave $P(r) = P_0 \exp(ikz)$ impinges on such a bubble with a frequency near its resonance, a spherical wave weighted by the incident wave amplitude, P_0 , and the scattering amplitude, $f = R_0 / \left(\left(\frac{\omega_M^2}{\omega^2} - 1 \right) - i\delta \right)$, is reradiated in the fluid. Here δ accounts for losses through viscosity, thermal conduction and radiation. The efficiency of scattering defined as the power radiated by the bubble over a unit incident intensity is then given by the so-called scattering cross section: $\sigma = 4\pi f^2 = 4\pi R_0^2 / \left[\left(\frac{\omega_M^2}{\omega^2} - 1 \right)^2 + \delta^2 \right]$. σ can exceed the geometrical cross section (i.e., πR_0^2) by a factor 100.

Phononic crystals are periodic composite materials consisting of periodically distributed scatterers in a matrix with high impedance contrast of mass densities and/or elastic moduli, which can give rise to band structures due to the periodic Bragg scattering.² Among all the components one can think of to create a phononic crystal, air bubbles in water were often presented as very promising candidates due to their huge monopolar (Minnaert) resonance. Numerical studies even predicted that crystals with air inclusions in a liquid should exhibit the widest band gaps ever reported.^{3,4} An example is given in Fig. 1 where we plotted the dispersion relation of a bubble phononic crystal made of air bubbles ($R_0 = 38 \mu\text{m}$) arranged on a simple cubic lattice in water: a huge gap opens above the Minnaert resonant frequency. This gap does not originate from Bragg scattering but rather from hybridization between the free space propagation mode and the bubble Minnaert resonance. As shown in,³ this gap survives positional disorder. The branch above the gap has a slope close to the water sound velocity: that is, wave propagation mostly takes place in water. The second Mie-type bubble frequency resonance gives rise to the three degenerated flat bands observed at 3 MHz.^{3,4}

^aElectronic mail: arnaud.tourin@espci.fr

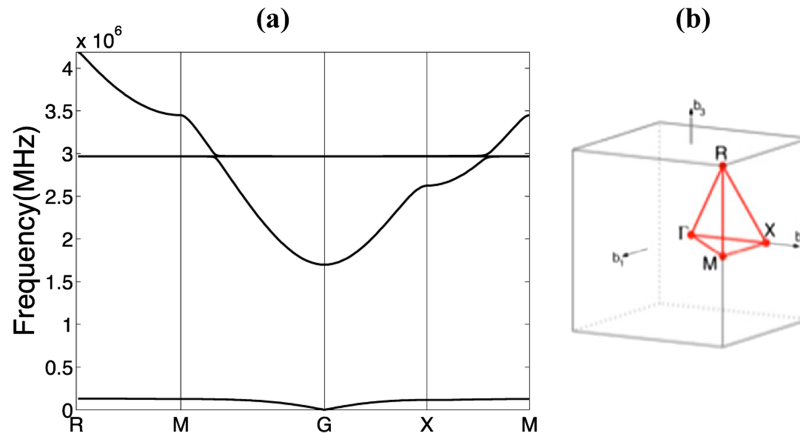


FIG. 1. (a) Dispersion relation of a bubble phononic crystal calculated by the Plane Wave Expansion method. The crystal consists of 38- μm -radius air bubbles arranged on a simple cubic lattice in water with a lattice parameter $a=300\text{ }\mu\text{m}$. The corresponding air volume fraction is 0.85 %. (b) Reciprocal lattice

II. PRACTICAL REALIZATION OF A BUBBLE PHONONIC CRYSTAL

No experimental evidence of such gaps were however reported since generating stable equally sized bubbles arranged on a crystal lattice in water is not an easy, if not impossible, task. We have recently shown that soft-lithography techniques could be used to circumvent these difficulties.⁵ The basic idea is to trap cylindrical air cavities in an elastomer matrix rather than spherical bubbles in a liquid. In that case, the shear modulus μ of the matrix shifts the air cavity resonance frequency ω_0 according to $\omega_0 = 1/R_0 \sqrt{(3B_g + 4\mu)/\rho_w}$. Providing that the matrix is soft enough, i.e., $\mu < B_g$, and the aspect ratio of the cylinders is close to unity, the cavities can be modeled as spherical bubbles of the same volume. In particular, the cavities still exhibit a low-frequency resonance, similar to the Minnaert bubble resonance. Thus bubbly soft elastic materials can be expected to exhibit acoustic properties quite analogous to bubbly liquids.

We have chosen PDMS as a soft matrix to comply with the soft-medium requirement. The samples were fabricated in RTV615 □Bayers Silicones□ using the standard soft-lithography procedure employed in microfluidics. We created 5-cm diameter molds with two-dimensional periodic arrangements of cylinders. A thin layer of PDMS (monomer and hardener with a 10:1 weight ratio) was then deposited on the mold by spin coating (50s at 100 rpm) and cured at 70 °C for 1 h. By stacking 4 patterned layers and closing the structure with a pure PDMS layer, we finally obtained a three-dimensional crystal. Two different molds were fabricated with different lattice constants. From these two molds, two one-layer crystals (see Fig2.a and Table I) and two four-layer crystals (see Fig2.b and Table I) were produced.

Ultrasonic measurements were carried out in a large water tank (Fig. 2.c). A piezoelectric transducer generated a short pulse that propagated through water, traversed the sample along z direction, and reached a receiving transducer. Here we have to point out that a perfect alignment from one layer to the other is difficult to ensure. Thus all measurements have been performed in normal incidence (propagation along z direction). The sample was placed in the far field of the transducers and, to reduce spurious signals coming from the edges, it was mounted on the aperture (4-cm diameter) of an acoustically opaque screen. It was checked that there was no ultrasonic reflection from the interface between two layers of plain PDMS, thus ensuring that our samples of stacked layers could be considered as 3D blocks of PDMS with air inclusions. We also measured the phase velocity of ultrasound in pure PDMS and found $v = 1.02\text{ mm}/\mu\text{s}$ in accordance with previously reported values.⁶ The transmission factor was obtained by calculating the ratio of the Fourier transforms of the signals acquired with and without the sample in the path of the acoustic beam. Two pairs of transducers were used, with central frequencies of 1 and 3.5 MHz respectively, allowing measurements of the transmission between 0.3 and 5 MHz.

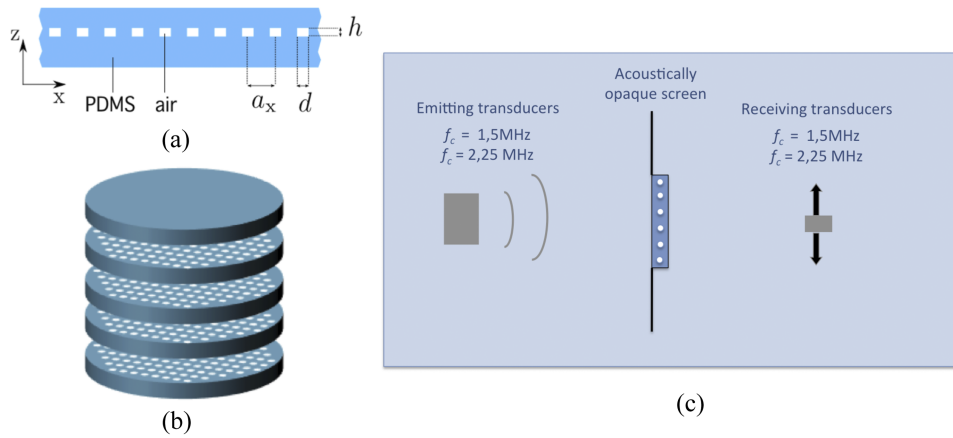


FIG. 2. (a) A one-layer crystal consists of an array of periodically arranged cylindrical air cavities in PDMS. (b) 3D phononic crystals were made by stacking four layers. The lattice constant along z will be denoted as a_z . (c) Experimental setup for measuring acoustic transmission. The sample was placed between two transducers, one acting as a source, the other as a receiver. Two pairs of transducers were used to cover the frequency range between 0.3 MHz and 5 MHz.

TABLE I. Lattice constants and bubble size for the 4 crystals used in this study.

Sample	a_z (μm)	$a_x = a_y$ (μm)	h (μm)	d (μm)	R (μm) Radius of the equivalent sphere
Crystal 1	One single layer	300			
Crystal 2	One single layer	200			
Crystal 3	475	300	50	78	38
Crystal 4	1150	300			

III. RESULTS AND DISCUSSION

We have first investigated the transmission through one layer of bubbles (Fig. 3). A minimum of transmission is found at 530 kHz for crystal 1 and 590 kHz for crystal 2, which is the signature of a hybridization gap (Fig. 3.a). Such a gap originates from the coupling between the propagation mode of the embedding medium and bubble resonances. Above resonance, each bubble scatters a wave that interferes destructively with the incident one, thus creating a gap in transmission. Compared to the individual Minnaert frequency of one bubble in PDMS (325 KHz), the position of the gap is shifted towards higher frequencies, all the more than the density of bubbles is larger as revealed by the comparison of the transmission through two samples with different lattice parameters (Fig. 3.a). Based on a model taking into account multiple scattering in the bubble layer, the position can be found to vary as $\omega_c = \omega_0 / \sqrt{1 - 2\sqrt{\pi}R/a_x}$ as a function of the lattice constant.⁷ The nature of the gap is verified by a comparison with a random sample, where the gap persists (Fig. 3.a). It can be further confirmed by analyzing the dispersion relation. The effective wave vector is largely imaginary and its real part exhibits a typical polariton-like behavior with a negative group velocity inside the gap (see Fig. 3.b). The gap allows the definition of a negative effective compressibility and makes a bubble layer a metamaterial that can be referred to as a bubble metascreen.⁸

Then we have studied the transmission through 4-layer crystals. Inspired by previous works including ours,^{5,9–12} our aim was to carefully study the interaction between hybridization and Bragg effects in the formation of the gap. We have first deliberately chosen a lattice parameter, $a_z = 475 \mu\text{m}$, for which hybridization and Bragg gaps overlap. That lattice parameter verifies $a_z = \lambda/4$, with $\lambda = 1.9 \text{ mm}$ the wavelength in PDMS. The corresponding crystal is labeled crystal 3 (see Table I).

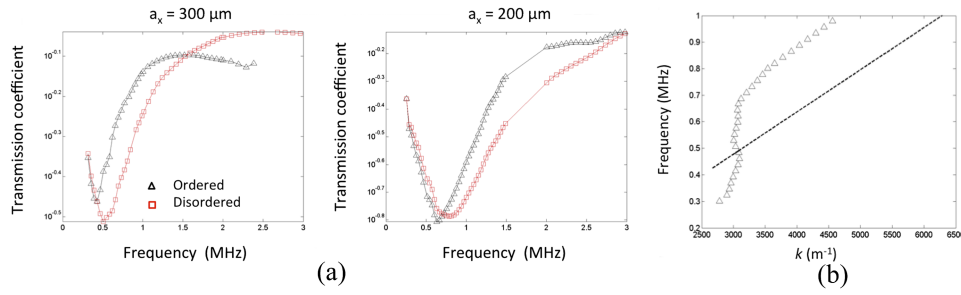


FIG. 3. (a) Acoustic transmission measured on crystals 1 (left) and 2 (right) and comparison with disordered distributions of the same bubbles with the same density. (b) Experimental dispersion relation of crystal 1. The dispersion in homogeneous PDMS is plotted as a dashed line. The interaction between the mode of the homogeneous PDMS and the bubble resonance gives rise to a S-shaped dispersion law typical of a polariton behavior.

The ultrasound transmission through that crystal (see solid circles in figure 4a) is found to be remarkably low for a sample whose thickness is less than 2mm and with an air volume fraction as low as 0.6%. It appears that the transmission around 0.5 MHz is lower than that would be predicted from the one-layer transmission (downward-pointing triangles in figure 4a) due to the additional effect of the Bragg gap. A second gap around 1.4 MHz is also observed. Figure 4 also gives the predictions inferred respectively from a 1D-layered model and a Multiple Scattering Theory (MST) code.^{5,13} Both take dissipation into account and give a satisfactory agreement with the experimental data. The layered model is a 1D description of the crystal in which each layer of bubbles is treated as a partially reflective layer with a reflection coefficient r and a transmission coefficient $t = 1 + r$ inferred from the model by Leroy *et al.*⁷ An iterative process then leads to the following expressions for the reflection R_{N+1} and the transmission T_{N+1} through $N+1$ thin layers separated by a distance a_z :

$$R_{N+1} = r + R_N \frac{t^2 e^{2ika_z}}{1 - R_N r e^{2ika_z}} \quad (1.a)$$

$$T_{N+1} = \frac{t T_N}{1 - R_N r e^{2ika_z}} \quad (1.b)$$

The hybridization character of the first gap remains predominant as seen on the dispersion curve (Fig. 5a and Fig. 5b). The second gap around 1.4 MHz is a pure Bragg gap (not observed for the one-layer crystal #1) characterized by a positive group velocity higher than that of pure PDMS (Fig. 5c). The group velocity would even tend to infinity for a sample of infinite size in the z -direction.

We have also plotted the dispersion curve in the first Brillouin zone (Fig. 6). Interestingly, the first gap does not open at the crossing of the first Brillouin zone, as it would be expected for

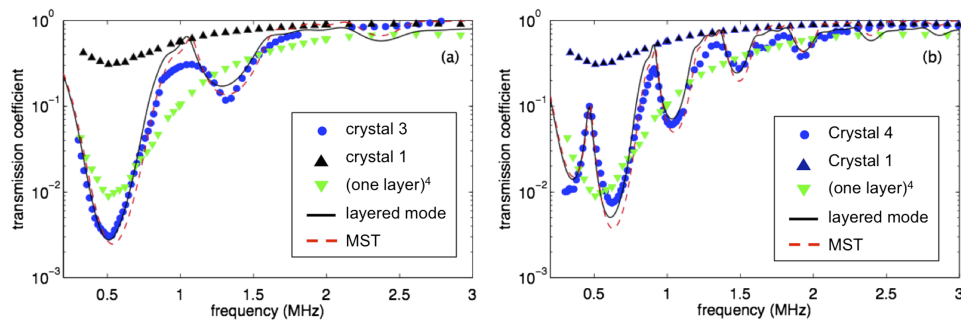


FIG. 4. (a) Transmission coefficients as a function of frequency for crystal 1 and 3. The additional effect of reflections between layers has to be taken into account to predict correctly the transmission. It can be done using our simple layered model. The MST calculation also fits the data. (b) Same for crystals 1 and 4. The reflections between layers now build a peak inside the hybridization gap.

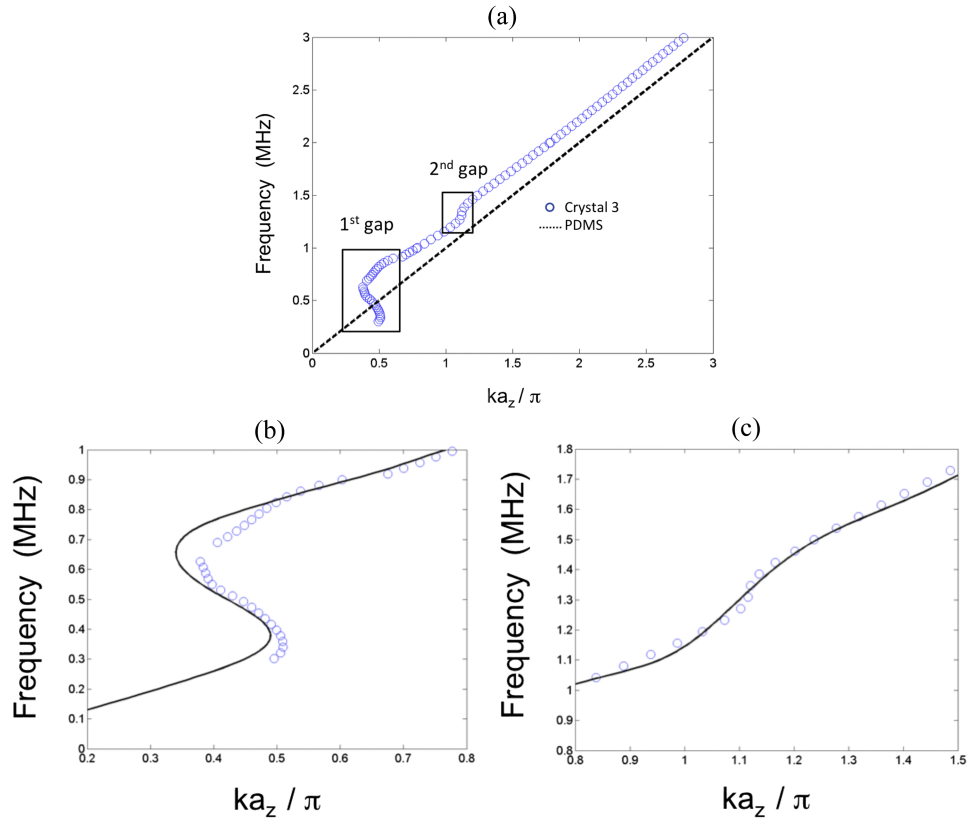


FIG. 5. (a) Experimental dispersion relation (frequency versus wavevector) of crystal 3. (b) Zoom on the region of the first gap (c) Zoom on the region of the second gap. Experimental data (blue circles) are well fitted with our one-layer model (Eq. 1.b).

a classical Bragg gap. The explanation for this result is that the Bragg condition must be modified when considering a strong reflector, such as a bubble layer near bubble resonance, instead of a low reflector such as an atomic layer in crystal. For continuity and energy conservation reasons, the transmission and reflection coefficients of one crystal layer always take the general form $t = A/(A - iB)$ and $r = iB/(A - iB)$, with A and B two real numbers. For a low reflector (case of an

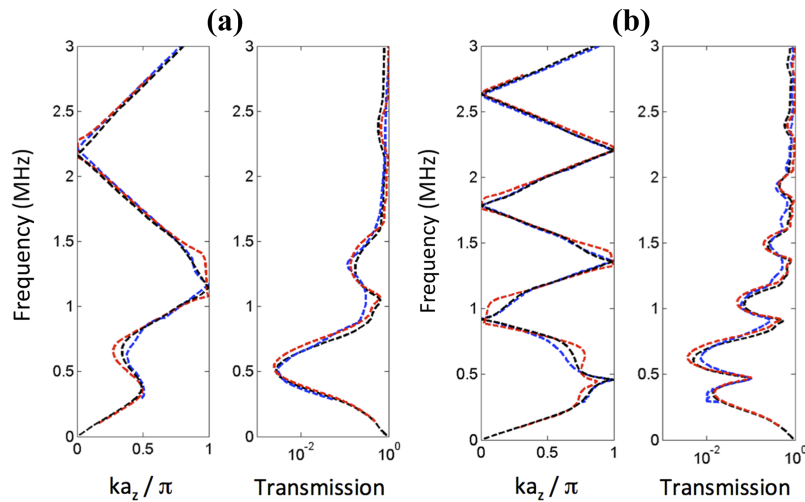


FIG. 6. Dispersion relations (frequency versus wavevector) of crystal 3 (left) and crystal 4 (right) plotted in the first Brillouin zone. Experimental data are well fitted by predictions from the one-layered model (in black) and MST code (in red).

atomic crystal layer), $B < A$, the wave is reflected with a phase shift $\pi/2$ and the Bragg condition writes $2ka_z = 2\pi$ like it is usual. For a strong reflector, $A < B$, and the transmission through one layer is accompanied with a phase shift of $\pi/2$, such that the Bragg condition now writes $2ka_z + \pi = 2\pi$, i.e., $a_z = \lambda/4$.

To further investigate the coupling between the two gaps, we built another sample referred to as crystal 4. This time its lattice constant a_z was chosen to correspond to a maximum in transmission at 530kHz, i.e., close to $\lambda/2 = 940\mu\text{m}$. As shown in figure 4.b, the Bragg reflections now build a peak in the hybridization gap, similarly to a resonant tunneling effect. Once again experimental data are well fitted by both the MST calculation and the layered model. As in the previous case, the dispersion relation plotted in the first reduced Brillouin zone (Fig. 6.b) reveals a behavior different from usual Bragg crystals for the first gap even if the S-like shape disappears. The other gaps exhibit a classical Bragg crystal behavior.

IV. CONCLUSION

We have reported on the fabrication of bubble phononic crystals that exhibit gaps combining two mechanisms: Bragg effects due to the periodicity of the structure and hybridization between the propagating mode of the embedding medium and bubble resonances. These two types of gaps have different behaviors. The hybridization gap survives disorder while the Bragg gap requires a periodic distribution of scatterers (along z axis). The distance between two bubble layers can be chosen to make the two gaps overlap. Interestingly, the resulting gap does not open at the crossing of the Brillouin zone, which can be explained by the transmission properties of a single bubble layer. The success of the layered model means that, at least to a first approximation, the hybridization gap only depends on the parameters of a single layer (a_x, a_y, h, d) whereas the Bragg gap is only governed by the distance a_z between layer. This simple description would probably break down if the wave were not normally incident on the crystal. Finally, we have shown that the distance between two bubble layers can also be chosen to build a resonant peak in the hybridization gap.

ACKNOWLEDGMENTS

We thank J. Page for fruitful discussions. This work was supported by LABEX WIFI (Laboratory of Excellence ANR-10-LABX-24) within the French Program “Investments for the Future” under Reference ANR-10-IDEX-0001-02 PSL*. We thank Direction Générale de l’Armement (DGA) for the financial support to Maxime Lanoy.

- ¹ M. Minnaert, *Philosophical Magazine* **16**(104), 235–248 (1933).
- ² M. S. Kushwaha, P. Halevi, L. Dobrzynski, and B. Djafari-Rouhani, *Phys. Rev. Lett.* **71**, 2022 (1993).
- ³ M. Kafesaki and E. N. Economou, *Phys. Rev. B* **52**, 13317 (1995).
- ⁴ M. S. Kushwaha, B. Djafari-Rouhani, and L. Dobrzynski, *Physics Letters A* **248**, 252 (1998).
- ⁵ V. Leroy, A. Bretagne, M. Fink, H. Willaime, P. Tabeling, and A. Tourin, *Appl. Phys. Lett.* **95**, 171904 (2009).
- ⁶ G. Delides and T. A. King, *J. Chem. Soc., Faraday Trans.* **2**(75), 359 (1979).
- ⁷ V. Leroy, A. Strybulevych, M. G. Scanlon, and J. H. Page, *Eur. Phys. J. E* **29**, 123 (2009).
- ⁸ A. Bretagne, A. Tourin, and V. Leroy, *App. Phys. Lett.* **99**, 221906 (2011).
- ⁹ T. Still, W. Cheng, M. Retsch, R. Sainidou, J. Wang, U. Jonas, N. Stefanou, and G. Fytas, *Phys. Rev. Lett.* **100**, 194301 (2008).
- ¹⁰ E. J. S. Lee and J. H. Page, *Proceedings of Symposium on Ultrasonic Electronics* **30**, 461 (2009).
- ¹¹ C. Croënne, E. J. S. Lee, H. Hu, and J. H. Page, *AIP Adv.* **1**, 041401 (2011).
- ¹² Y. Achoufi, A. Khelif, S. Benhabane, L. Robert, and V. Laude, *Phys. Rev. B* **83**, 104201 (2011).
- ¹³ I. E. Psarobas, A. Modinos, R. Sainidou, and N. Stefanou, *Phys. Rev. B* **65**, 064307 (2002).